Rampanelli Elena (Orcid ID: 0000-0002-7742-0092)

De Borst Martin (Orcid ID: 0000-0002-4127-8733)

BONTHRON EDITED – ORIGINAL ARTICLE

Excessive dietary lipid intake provokes an acquired form of lysosomal lipid storage disease in the kidney

Running title: Diet-induced renal phospholipidosis and associated damage

Elena Rampanelli[1,*], Peter Ochodnicky[1,*], Johannes P.C. Vissers[2], Loes M. Butter[1], Nike Claessen[1], Alessia Calcagni[3], Lotte Kors[1], Lee A. Gethings[2], Stephan J.L. Bakker[4], Martin H. de Borst[4], Gerjan J. Navis[4], Gerhard Liebisch[5], Dave Speijer[6], Marius A. van den Bergh Weerman[1], Bettina Jung[7], Jan Aten[1], Eric Steenbergen[8], Gerd Schmitz[5], Andrea Ballabio[3], Sandrine Florquin[1], Johannes M.F.G. Aerts[9], Jaklien C. Leemans[1]

[1] Pathology Department, Academic Medical Center, University of Amsterdam, Amsterdam, The Netherlands.

[2] Waters Corporation, Wilmslow, United Kingdom.

[3] Telethon Institute of Genetics and Medicine (TIGEM) & Medical Genetics, Department of Translational Medicine, Federico II University, Naples, Italy.

[4] Department of Internal Medicine, Division of Nephrology, University Medical Center Groningen, University of Groningen, Groningen, The Netherlands.

[5] Institute for Clinical Chemistry and Laboratory Medicine, University Hospital of Regensburg, Regensburg, Germany.

[6] Department of Medical Biochemistry, Academic Medical Center, University of Amsterdam, Amsterdam, The Netherlands.

[7] Division of Nephrology, University Hospital of Regensburg, Regensburg, Germany.

This article has been accepted for publication and undergone full peer review but has not been through the copyediting, typesetting, pagination and proofreading process which may lead to differences between this version and the Version of Record. Please cite this article as doi: 10.1002/path.5150

[8] Department of Pathology, RIMLS, RIHS, Radboud University Medical Center, Nijmegen, The Netherlands.

[9] Department of Biochemistry, Leiden Institute of Chemistry, Leiden University, Leiden, The Netherlands.

[*] These authors contributed equally.

Conflict of interest

The authors declare that they have no conflict of interest.

ABSTRACT

Obesity and dyslipidaemia are features of the metabolic syndrome and risk factors for chronic kidney disease. The cellular mechanisms connecting metabolic syndrome with chronic kidney disease onset and progression remain largely unclear. We show that proximal tubular epithelium is a target site for lipid deposition upon overnutrition with a cholesterol-rich Western-type diet. Affected proximal tubule epithelial cells displayed giant vacuoles of lysosomal or autophagosomal origin, harbouring oxidized lipoproteins and concentric membrane layer structures (multilamellar bodies), reminiscent of lysosomal storage diseases; lipidomic analysis revealed renal deposition of cholesterol and phospholipids, including lysosomal phospholipids. Proteomic profiles of renal multilamellar bodies were distinct from those of epidermis or lung multilamellar bodies and of cytoplasmic lipid droplets. Tubular multilamellar bodies were observed in kidney biopsies of obese hypercholesterolaemic patients, and the concentration of the phospholipidosis marker di-docosahexaenoyl (22:6) bis(monoacylglycerol) phosphate was doubled in urine from individuals with metabolic syndrome and chronic kidney disease. The enrichment of proximal tubule epithelial cells with phospholipids and multilamellar bodies was accompanied by enhanced inflammation, fibrosis, tubular damage markers and higher urinary electrolyte content. Concomitantly to the intralysosomal lipid storage, a renal transcriptional response was initiated to enhance lysosomal degradation and lipid synthesis. In cultured proximal tubule epithelial cells, inhibition of cholesterol efflux transport or oxysterol treatment induced effects very similar to the *in vivo* situation, such as multilamellar body and phospholipid amassing, and induction of damage, inflammatory, fibrotic and lipogenic molecules. Onset of phospholipidosis onset in proximal tubule epithelial cells is a novel pathological trait in metabolic syndrome-related chronic kidney disease, and emphasizes the importance of healthy lysosomes and nutrition for kidney wellbeing.

Keywords: diet, lipids, kidney, chronic kidney disease, multilamellar bodies, lysosomal storage disease, lysosome, metabolism, inflammation, fibrosis

Introduction

In the current obesity epidemic, increasing attention has been given to the obesity-related diseases, atherosclerosis, diabetes and metabolic syndrome (MetS). Emerging evidence indicates that MetS individuals are prone to chronic kidney diseases (CKD) and end-stage renal diseases (ESRD). A systematic meta-analysis based on 25 general population cohort studies demonstrates that obesity confers a significantly higher risk of kidney disease compared to normal-weight individuals [1]. In addition, two large cohort studies in Japan and in the United States linked an increased risk for ESRD with high body-mass index (BMI) [2, 3] independently of hypertension and diabetes [2-6]. Remarkably, visceral obesity also puts lean subjects at risk of CKD [7, 8]. The association between MetS and CKD becomes particularly relevant in renal transplantation, as MetS appearance adversely affects allograft survival and long-term function [9].

Despite such associations between MetS and CKD, the etiological role of MetS and obesity in CKD development and progression remains unclear, due to the complexity and bidirectionality of the relationship between the two medical conditions [10]. Nevertheless, the description of ectopic fat deposition in kidneys and the strong interrelation between obesity (particularly BMI) and ESRD suggest a role for fat accumulation *per se* in the initiation of renal dysfunction or in the progression of existing renal disease [11, 12]. Several studies indeed hint at a causal relationship: (a) weight loss ameliorates proteinuria in overweight patients affected by chronic proteinuric nephropathies; (b) the rates of allograft dysfunction and acute rejection episodes are higher for obese living kidney donors; (c) inhibition of 3-hydroxy-3-methylglutaryl-coenzyme A reductase (HMGCR), the rate-limiting enzyme in cholesterol biosynthesis, improves proteinuria and reduces renal function loss; (d) low-carbohydrate and low-fat diets exert beneficial effects on renal function in obese individuals [13-17]. Altogether, these reports strongly indicate a lipid-mediated effect in initiating renal dysfunction or

injury. In this regard, most of the lipotoxic effect of renal lipid overload linked to obesity and MetS and kidney dysfunction has been attributed to renal steatosis through free-fatty acid (FFA) and triglyceride (neutral lipids) accumulation within cytoplasmic lipid droplets (LDs) [12, 18, 19]. Here, we report the accumulation of free cholesterol (FC) and phospholipids (polar lipids) within multilamellar organelles of lysosomal origin (phospholipidosis) inside renal proximal tubular epithelial cells (PTEC) following Western-diet (WD) feeding. A similar excessive storage of complex polar lipids has been disclosed in PTEC in lysosomal storage diseases, caused by defects in lysosomal lipases or lysosomal lipid transport proteins [20].

Material and Methods

Animal studies

Male wild-type C57BL/6 mice (Charles River) were subjected to control diet (4021.84, AB Diets), Western diet (4021.83, AB Diets) or water enriched with 15% (w/v) fructose (Sigma Aldrich) *ad libitum* for 16 weeks [21]. GFP-LC3 transgenic mice [22, 23] were fed Western diet. Kidneys from $Npc1^{nih/nih}$, Gla^{tm1Kul}/Y, ob/ob mice and 88-week-old mice were used for transmission electron microscopic (TEM) imaging [24-27]. All procedures were approved by the Animal Care and Use Committee of the Academic Medical Center Amsterdam.

Cell culture and isolation of multilamellar bodies (MLBs)

HK2 and IMM-PTEC were cultured in DMEM/F12 supplemented with ITSe, triiodothyrionine, hydrocortisone and prostaglandin E1 (Sigma-Aldrich), plus interferon-ϒ for IMM-PTEC (PROSPEC) [28]. MLBs were isolated by homogenization and sucrose gradient fractionation; MLBs were recovered at the interface between 0.4 M and 0.35 M sucrose. Urine MLBs were purified by ultracentrifugation [29]

Lipidomics and proteomics

Lipids were isolated by chloroform/methanol extraction and quantified by ESI-MS/MS [30-32]. Sphingolipids were butanol-extracted and analysed by LC-MS/MS [33-35]. GC-MS Solution Software was used for data acquisition and processing [36]. Urine di-docosahexaenoyl (22:6) bis(monoacylglycerol) phosphate (di-22:6-BMP) content was determined by HPLC-MS [37, 38].
For LC-MS proteomics, samples were denatured and digested, following by Nanoscale LC separation of tryptic peptides. MS data were acquired in triplicate in ion mobility enabled data independent analysis mode [39] using a Synapt G2-S*i* instrument (Waters Corporation). ISOQuant was applied for integrated quantitative analysis of data from multiple LC-MS [40, 41]. Reactome, BLAST2GO, GO

terms and KEGG pathway annotation analyses were used for pathway/gene ontology annotation [42-44].

Patient study

Urine samples belong to the TransplantLines cohort (ClinicalTrials.gov Identifier: NCT02811835, University Medical Center Groningen, The Netherlands) [45-48] Control samples were obtained from transplant donors and the disease group was selected on basis of CKD clinical diagnosis and presence of clinical parameters matching MetS World Health Organization criteria (hypertension, BMI, plasma cholesterol and triglycerides). The transmission electron microscopy (TEM) images shown in supplementary material, Figure S5 were selected from screening 69 biopsies of nephrotic syndrome patients from the University Hospital of Nijmegen, The Netherlands; the images of Figure 5E are derived from obese hypercholesterolaemic patient renal biopsies collected at the Academic Medical Center of Amsterdam, The Netherlands.

Statistics

Statistics was performed using One-Way ANOVA and Dunnett's tests; Mann-Whitney U test and Spearman rank correlation. Data are presented as mean and SEM; $p < 0.05$ was considered significant.

Results

Accumulation of polar lipids/phospholipids and free-cholesterol in murine proximal tubular epithelial cells upon Western-type diet feeding

Feeding mice for 16 weeks a Western-type diet (WD) containing 0.15% cholesterol and providing 43% energy from fat *vs.* a control diet (CD), in which 11% of energy comes from fat, leads to a prominent cytoplasmic vacuolization of renal tubular epithelial cells (Figure 1A,B). In all kidneys from WD-fed mice, the vacuoles were located in the proximal tubules S2/S3 segments (not in S1) and absent in distal tubular, endothelial or glomerular cells (Figure 1A, and supplementary material, Figure S1A). By staining kidney sections for the lipid droplet marker perilipin-2 [49, 50], we found numerous small LDs along the tubular cell basolateral membrane after WD-feeding; however, the large, more apically located, vacuoles were all negative for perilipin-2 (Figure 1C). Remarkably, these vacuolized tubules were enriched in phospholipids and free-cholesterol, as shown by Nile red and filipin staining, respectively (Figure 1D,E). Accordingly, quantitative lipidomics analysis of renal tissues from mice subjected to WD revealed an increase in several lipids, including free-cholesterol (FC), fatty acids (FA), several phospholipids and sphingolipids (Figure 1F).

As human studies showed that obesity increases the incidence of a distinct obesity-related glomerulopathy (ORG) [51-53], the extent of glomerular lesions (mesangial cell proliferation, mesangial matrix expansion and mesangiolysis) after WD feeding was evaluated. However, no significant alterations were observed in the glomerular compartment between CD and WD groups (supplementary material, Figure S1B). Thus, although kidneys are generally regarded as non-highly active metabolic organs, we show that tubular epithelial cells are sites of profound lipid deposition within large vacuoles during lipid overnutrition.

Features of acquired lysosomal storage disease in kidneys exposed to lipid overloading

Transmission electron microscopy revealed that these tubular vesicles contained lots of concentric thin electron-dense lamellae surrounded by a limiting membrane (Figure 2A). These structures reached a maximum diameter of 8-9 µm and ultrastructurally resembled the multilamellar bodies (MLBs) that we and others found in kidneys from mice with lysosomal storage diseases such as Fabry and Niemann-Pick type C [24, 54] (supplementary material, Figure S2A). In line with studies associating aging with lysosomal impairment [55], aged mice also presented MLBs. As after WD feeding, subjecting mice to high-fat diet (HFD) resulted in MLB formation in PTEC (supplementary material, Figure S2A). In contrast, leptin-deficient (ob/ob) mice on a regular diet and Wt mice given *ad libitum* water enriched with 15% fructose for 16 weeks have hardly any renal MLBs (supplementary material, Figure S2B, S2C). This implies that the massive expansion of MLBs in PTEC is a specific reaction to excessive dietary lipid intake, and not generally to any kind of overnutrition.
Next, we discovered that lysosomal and autophagy markers, LIMP-2, CD63, p62 and LC3 [56], were present in the vacuole delimiting zone in WD-PTEC (Figure 2A,B). To directly monitor autophagy, GFP-LC3 transgenic mice were fed a WD for 16 weeks; we found that both LIMP-2 and GFP-LC3 co-localized at the vacuole limiting membrane and Western diet dramatically increased renal GFP-LC3 puncta formation (Figure 2C). This suggests a lysosomal/autophagic origin (autolysosomes) [57] of renal diet-induced MLBs, similarly to what is described in lysosomal storage diseases [20].
We next used laser-capture microdissection (LCM) technology to obtain a histologically pure cell population enriched in vacuolized PTEC for RNA transcript profiling. The expression of lysosome- and lipid metabolism-associated genes was enhanced in response to high-fat/cholesterol feeding in vacuolized proximal tubules (Figure 2D). Indeed, the transcription of genes encoding LIMP-2 and the master regulator of lysosomal function transcription factor EB (TFEB) showed a trend towards increased expression upon overnutrition ($p = 0.057$) and the gene expression of the lysosomal

enzymes acid ceramidase *Asah1* (N-acylsphingosine amidohydrolase 1) and acid sphingomyelinase *Spmd1* (sphingomyelin phosphodiesterase 1) was significantly upregulated in WD-vacuolized tubules [58, 59]. Furthermore, the lipogenic transcription factors sterol regulatory element-binding protein 2 and 1c (*Srebp2*, *Srebp1c*) and their target genes *Ldlr* (low-density lipoprotein receptor) and *Fas* (fatty acid synthase), respectively, were strongly induced in lipid-enriched tubules [60, 61] (Figure 2D). Altogether, our findings disclose the importance of tubular lysosomes in the renal response to WD feeding and the acquisition of a "lysosomal storage disease phenotype" in PTEC upon diet-derived lipid overload.

Finally, we found that renal MLB formation is likely to be driven by lipoprotein uptake, since WD-induced renal vacuoles harbour lipoproteins, including oxidized lipoproteins, and LDLR (Figure 2E).

Renal and urinary MLBs have a unique proteomic footprint

As MLBs from other organs are known to be released into the extracellular space [54], we wondered whether MLBs could be secreted by PTEC. MLBs can be detected by TEM in urine of mice fed a WD (Figure 3A). In addition, immortalized proximal tubular epithelial cells (IMM-PTEC) secreted extracellular vesicles in a lysosomal storage disease-like state, as proven by the detection of the flotillin-2 extracellular vesicle marker [62] in the supernatant of IMM-PTEC treated with U18666A, an inhibitor of cholesterol trafficking out of lysosomes, largely used to reproduce *in vitro* the NPC1 disease [63-65] (Figure 3B).

To better characterize MLBs, proteomic analysis was performed on MLBs isolated from kidneys and urine of WD-fed mice or U18666A-stimulated IMM-PTEC (supplementary material, Figure S3A-C). We identified 526 proteins (supplementary material, Excel spreadsheet S1); Figure 3C shows the most abundant proteins detected in kidneys, urine and IMM-PTEC upon metabolic overloading. Many of these proteins have been identified as located within extracellular exosomes, and some, such as

GGT1 (gamma-glutamyltransferase 1), ATPA1 (ATPase, Na+/K+ transporting, alpha 1 polypeptide), and ALDOB (aldolase B, fructose-bisphosphate) have high (though not exclusive) renal expression, (www.ncbi.nlm.nih.gov/gene). In addition, kidney MLBs express proteins involved in lipid cellular uptake and trafficking, such as megalin [66, 67], sterol carrier protein 2 (SCP2) [68, 69], Hsp90 [70], legumain (LGMN) [71], Na^+/H^+ exchange regulatory cofactor 3 (NHRF3) [72], and fatty acid-binding proteins (FABPs), albumin and apolipoprotein E [73].

Proteomics also revealed the presence of lysosomal proteins and proteins normally located in other organelles and cellular compartments, such as cytoskeleton, mitochondria and plasma membrane (Figure 3D and supplementary material, Figure S4). Reactome pathway-based analysis show that metabolism-related pathways are among the most enriched pathways (supplementary material, Figure S3D, highlighted in yellow) associated with the MLB proteome. This is in line with the known lysosomal functions in cellular clearance and nutrient/energy sensing [74, 75] and the above described data indicating that lysosome-derived MLBs are part of a metabolic cellular adaptation to lipid overload.

It is to be noted that we used a common organelle isolation procedure based on gradient-density centrifugation, as employed by others for MLB isolation [76, 77]. Although this method is not completely contamination-free, it is the only one suitable for organelle isolation from tissues, in contrast to isolation from cell lines, which can be engineered to stably express a tagged organelle-specific marker. Comparison of the renal MLB proteome with published data from proteomics of lysosome-related organelles (LRO), lung/epidermis-derived MLBs and lipid droplets from enterocytes, adipocytes or hepatocytes [76-81] revealed that renal MLBs have a unique protein profile, as shown by frequency/hierarchical clustering analysis (Figure 4). Indeed, most proteins were identified solely in renal MLBs, but not in lung/skin MLBs or LDs (supplementary material, Excel spreadsheet S2 and

Table S1), indicating that they are distinct organelles. However, comparing GO annotation and pathways analyses of all seven sets of proteomes revealed that most of the detected proteins share similarities in general function such as catalytic activity and binding and participation in metabolic processes (supplementary material, Figure S5).

Oxysterols and impaired cholesterol trafficking cause MLB formation, disruption of lysosome homeostasis and induction of cholesterogenesis genes

By means of *in vitro* assays with IMM-PTEC, we demonstrate that the same multilamellar structures observed *in vivo* upon nutrient overload appear in PTECs after exposure to U18666A, oxidized LDL (oxLDL) and 7-ketocholesterol (7KC), which is the major oxidation product of cholesterol and among the most common oxysterols found in food [82] (Figure 5A). Accordingly, IMM-PTEC treatment with U18666A, oxLDL or 7KC elevates the intralysosomal phospholipid content and the expression of LIMP-2, as well as their colocalization (Figure 5B). Furthermore, oxysterols increase expression of both LIMP-2 and the autophagy adaptor p62 [56, 83] (Fig S2D). Altogether, the *in vitro* data validate the lysosomal origin of the MLB/vacuole organelles seen *in vivo* and suggest an etiological role of cholesterol overload in the disruption of lysosomal homeostasis.

Since the maintenance of a proper acidic pH is fundamental for the digestion of lysosomal cargo, including lipids [84], we studied the lysosomal acidification rate and found that U18666A, oxLDL and 7KC all increased lysosomal pH. Chloroquine was used as a positive control to inhibit lysosome acidification [85] (Figure 5C).

Lastly, tubular phospholipidosis was accompanied by internalization of cell surface free cholesterol and an increase in intracellular bismonoacylglycerophosphate (BMP), an atypical phospholipid specific for the (endo)lysosomal compartment involved in intracellular cholesterol transport [86] (Figure 5D). Besides, BMP expression overlapped with the sites of phospholipidosis in U18666A-

treated human PTECs (Figure 5E). Finally, the gene expression of *Srebp2*, *Ldlr* and *Hmgcr*, the rate-controlling enzyme in cholesterol synthesis [60], were all significantly upregulated by U18666A in IMM-PTEC, whereas the gene expression of the lysosomal phospholipase A2 was downregulated (Figure 5F).

Altogether, these data indicate that metabolic overloading of PTECs disrupts lysosomal homeostasis and reprograms cells towards the onset of anabolic pathways.

Diet-mediated lipid overload of tubular cells instigates tubular damage, inflammation and collagen deposition in mice, and promotes formation of lipid-rich MLBs in human TECs

To expand our view of the effects of overfeeding on kidney health and function, changes in damage, inflammatory and fibrotic parameters in kidneys were examined. Strikingly, after high-fat/cholesterol feeding, the expression of the sodium-glucose co-transporter 2 (SGLT2) at the apical membrane of proximal tubules almost vanished and concomitantly the proximal tubule injury marker KIM-1 (kidney injury molecule-1) [87] was induced in PTECs. The kidneys of WD-fed mice also show macrophage infiltration and collagen deposition (Figure 6A). The gene expression of *Sglt2* was significantly diminished in WD kidneys, whereas the transcription of genes encoding MCP-1 (monocyte chemoattractant protein-1), TGF-β (transforming growth factor-β) and CTGF (connective tissue growth factor) was augmented (Figure 6B). Accordingly, *in vitro* stimulation of IMM-PTEC with U18666A or 7KC provided similar results, with a reduced gene expression of the transporters *Sglt2* and *Atp1a1* (ATPase Na+/K+ transporting subunit α 1) and an increased expression of *Mcp1*, *Kim1*, *Tgfb1*, *Ctgf* (Figure 6C). In addition, WD feeding caused higher urinary concentrations of electrolytes that are normally reabsorbed from the tubular lumen after glomerular filtration (Figure 6D). These data strongly indicate that lipid-rich diets can provoke kidney disease as tubular injury and

malfunction, inflammation and collagen deposition are all key features of renal dysfunction and pathology [88].

To translate our *in vivo* and *vitro* findings to human obesity-related nephropathology, kidney biopsies and urine samples from obese and lean individuals were used. In the presence of obesity and hypercholesterolaemia, human PTEC display LIMP-2-positive vacuoles, BMP accumulation and MLBs (Figure 6E). In addition, patients affected by nephrotic syndrome, characterized by elevated serum levels of total cholesterol, LDL cholesterol, and lipoprotein(a) [89], present MLBs in renal tubules (supplementary material, Figure S6A), emphasizing the potential role of hyperlipidaemia in kidney MLB genesis. MLBs were also present at the brush border of tubular cells (supplementary material, Figure S6B) and in the tubular lumen (supplementary material, Figure S6C), which together with the detection of MLBs in urine (Figure 3A), strongly suggest that MLBs are excreted by TEC into the urinary space. Interestingly, we also found that the urinary concentration of di-22:6-BMP, a reliable marker for tissue-phospholipidosis [90], is much higher in the urine of a small cohort of individuals affected by CKD and MetS (Figure 6F) and shows a moderate positive correlation with the total albumin urinary content (Figure 6G). These findings imply that renal phospholipidosis also takes place in humans with metabolic/lipid disorders.

Discussion

Although a number of investigators have outlined the "renal lipotoxicity" hypothesis, the role of lipids *per se* as promoters of renal injury remains largely elusive and hard to prove, particularly in humans [91]. Altogether, our data indicate that excessive dietary lipid intake (and not overnutrition *per se*) cause the development of an "acquired lysosomal storage disease" in the kidney epithelium. Cholesterol/fat-rich Western diet induces large vacuoles enriched in free cholesterol, fatty acids and phospholipids and a robust MLB biogenesis in S2/S3 proximal tubules. Intratubular MLBs display lysosomal or autophagolysosomal origin and express the lysosome-bound BMP glycerolipid, resembling the features of lysosomal storage disease and oxLDL-loaded macrophages [54, 86]. Besides this, we detected MLBs in urine and found a striking excretion of the lysosomal di-22:6-BMP in urine of individuals affected by MetS and CKD. The lack of vacuoles, thus MLBs, in PTEC of S1 segment can be explained by their well-developed endo-lysosomal apparatus [92] and greater lysosomal volume and enzymatic activity compared to S2/S3 PTEC [93-96].

Although we cannot completely exclude MLB leakage from damaged TEC into urine, TEC-mediated MLB secretion seems more likely, in light of the known MLB secretion in other organs [54] and of our TEM-based observations of intact MLBs within TEC brush border. Accordingly, urine and kidney MLBs contain identical proteins, many of which are reported to be present in exosomes, and some of the MLB proteins (i.e. GGT1, ATPA1, ALDOB) with the highest relative abundance are also highly expressed in kidneys. In addition, the identification of proteins known to participate in lipid uptake and lipid intracellular trafficking within kidney-derived MLB strengthen our hypothesis of cholesterol/lipid-driven MLB formation, e.g. megalin (receptor for albumin-FA/LDL), SCP2 (intracellular cholesterol movement), Hsp90 (stabilization of NCP1); LGMN (lysosomal protein degradation), NHRF3 (maintenance of expression and function of the HDL receptor SR-BI),

apolipoprotein E (major cholesterol carrier), albumin and FABP suggest their uptake and incorporation in MLBs [66-73]. Thus, renal MLBs appear to be active organelles involved in storage of excessive lipids and secretion as urinary products; in kidneys, MLBs seems to act as a defence mechanism against lipid nephrotoxicity by sequestering and excreting surplus lipids.

Treatment of IMM-PTEC with 7KC hydroxysterol, oxidized-LDL and cholesterol trafficking inhibitor U18666A provoked tubular alterations very similar to the *in vivo* tubular changes, suggesting an etiological role of oxLDL/oxysterols in the obesity-related renal disease. Indeed, WD-induced tubular vacuoles contained LDLR and oxidized lipoproteins, which are more abundant in obesity [97]. Apolipoprotein E, FABP, albumin and megalin were detected in MLBs by proteomics; thus several lipotoxic molecules may promote lysosomal lipid storage development in our model, besides oxysterols. Besides oxysterols and lipoproteins, other lipotoxic molecules may account for lysosomal dysfunction and lipid-rich vacuole generation in PTEC. In agreement, Kuwahara *et al.* attributed the appearance of cytosolic vacuoles in PTEC following HFD-feeding to megalin-mediated FA endocytosis [67]. Nevertheless, autophagy is very likely implicated in "renal lysosomal storage disease" as we showed with GFP-LC3 WD-fed mice; consistent with this, autophagic flux contributes to the physiological production of MLBs in lung type II alveolar cells [98]. Although autophagy is regarded as a protective mechanism that contributes to lipid catabolism by delivering LD content to lysosomes (lipophagy) [99, 100], the rise in lysosomal pH observed in our *in vitro* model may block lipophagy through inhibition of pH-sensitive lysosomal hydrolases.

Interestingly and controversially, WD feeding initiated a transcriptional response in lipid-enriched vacuolized tubules, characterized by the up-regulation of genes accountable for lysosome biogenesis and function and concomitantly of genes responsible for cholesterol and FA synthesis. The enhanced gene expression of *Tfeb* itself together with *Asah1* attests to TFEB activation and nuclear relocation,

which leads to enhance autophagic and lysosomal lipolytic processes [58, 59]. This regulation is probably an adaption of cells to prevent lipotoxicity; indeed, overexpression of TFEB in liver protects against diet-induced obesity and MetS [101].

The increased expression of SREBP-1/2 by dietary lipid challenge is likely to sustain intratubular lipid accumulation during persistent overnutrition, since they upregulate genes for FA and cholesterol synthesis, respectively [60]. Upon lipid overload, phospholipids and cholesterol remain engulfed in lysosomes; therefore, less cholesterol is likely to be transported to the endoplasmic reticulum, where SREBPs reside and are suppressed by the cholesterol content, as cholesterol-induced suppression of SREBP activation vanishes and SREBP target genes are upregulated [60, 102]. Accordingly, we showed that inhibition of cholesterol transport with U18666A in TEC resulted in increased transcription of *Srebp2* and of its target genes *Hmgcr* and *Ldlr* [60, 61, 102].

The increased urinary electrolytes and the appearance of damage, inflammatory and fibrotic markers in WD-kidneys and in U18666A/7KC-treated IMM-PTEC provide an important causal link between kidney pathology and overnutrition. In fact, even though several epidemiological studies have proven a significant association of kidney dysfunction with obesity, dyslipidaemia and high BMI [2, 6, 103, 104], a direct detrimental impact of overnutrition and excessive metabolic loading of kidney cells on kidney health and function has been difficult to prove and is not yet established by scientific evidence.

Bis(monoacylglycerol)phosphate (BMP) is an atypical phospholipid localized mainly at the inner membrane of lysosomes, where its negative charge (due to the acidic pH) helps adherence of positively charged polycationic enzymes and activator proteins, thereby promoting hydrolysis/degradation [105]. Importantly for a translational aspect, the tissue phospholipidosis marker di-22:6-BMP [90, 106] was increased in urine specimens of individuals affected by CKD and

MetS, and urinary BMP levels positively correlated with albuminuria rates within the group of patients with obesity, dyslipidemia and CKD. Furthermore, BMP was shown to colocalize with intracellular phospholipidosis and vacuolization sites and lysosomes in murine/human PTEC. Future studies with larger cohorts would aid assessment of the potential of urinary di-22:6-BMP as a prognostic marker for MetS/obesity-mediated renal disease.

Inflammation and fibrosis are hallmarks of progressive renal disease [107]. In kidneys, MCP-1 was found to be increased as early as one week after initiation of high fat diet feeding [108]. This together with our *in vitro* findings (48h-treatment with U18666A, oxLDL, or 7-KC) suggests that proximal TEC can produce this chemokine at a very early stage upon metabolic challenge, possibly contributing to the macrophage infiltration observed in WD-fed mice. The induction of fibrotic markers in the kidney in the context of hypercaloric diet was previously reported [108-111]. Interestingly, the upregulation of SREBPs has a role in kidney fibrosis development, as shown by studies with SREBP-1c-deficent mice and SREBP-1a transgenic mice [12, 112]. Importantly, a recent report highlights the role of lysosomes and autophagy in renal lipotoxicity [113], while another reports enlarged vacuoles and multilamellar inclusions within PTEC following high fat diet [110]. We show that a high-cholesterol WD provokes equal pathological alterations in proximal tubules. Among the lipids found accumulated in kidneys after WD feeding, the sphingolipid ceramide and its metabolites, such as ceramide-1-phosphate (C1P) and sphingosine, warrant particular attention, due to their pro-inflammatory properties, which may favour renal inflammation [114, 115].

Altogether, our study shows that phospholipidosis in kidneys is a novel pathological pathway in obesity-related kidney disease and brings attention to the lysosomal compartment of renal tubules as potential target site for intervention/preventive approaches against MetS-induced nephropathy. It provides a rationale for screening individuals with obesity or metabolic syndrome, for kidney

dysfunction and phospholipidosis, *e.g.* with proton magnetic resonance spectroscopy [116], to identify early-stage CKD patients, who can still profit from changes in diet, lifestyle and lipid-lowering therapies.

Acknowledgements

This study was supported by the Netherlands Organization for Scientific Research (NWO Vidi and ASPASIA #91712386) and by EU-funded "LipidomicNet" project (#202272). We thank Per W.B. Larsen (Electron Microscopy Core, AMC, Amsterdam, The Netherlands) for technical assistance.

Author contributions

Elena Rampanelli and Peter Ochodnicky contributed to the design of the research, performed experiments, analyzed and interpreted data and wrote the paper. Johannes P.C. Vissers and Lee A. Gethings performed LC-MS proteomics analysis, Gerhard Liebisch performed MS lipidomics analysis. Alessia Calcagni, Lotte Kors and Gwen J. Teske conducted *in vivo* experiments. Loes M. Butter and Nike Claessen conducted laboratory work. Marius A. van den Bergh Weerman and Jan Aten conducted sample preparation and TEM imaging. Dave Speijer helped isolating multilamellar bodies. Bettina Jung helped in sample collection. Stephan J.L. Bakker, Martin H. de Borst, and Gerjan J. Navis collected and provided human urine samples and clinical data. Eric Steenbergen provided renal biopsies for TEM imaging and the corresponding patient clinical diagnosis. Gerd Schmitz contributed with background knowledge on lysosomal storage disease, phospholipidosis and lipid droplets. Johannes M.F.G. Aerts, Andrea Ballabio, Sandrine Florquin, Jan Aten, Stephan JL Bakker, Martin H de Borst, and Gerjan J Navis helped in interpreting and discussing data and reviewed the manuscript. Jaklien C. Leemans led the research project and contributed to the conception and design of the work. All authors discussed the results and participated in drafting or revising the article.

References

1. Wang Y, Chen X, Song Y, Caballero B, *et al.* Association between obesity and kidney disease: A systematic review and meta-analysis. *Kidney Int* 2008; **73**: 19-33.
2. Iseki K, Ikemiya Y, Kinjo K, *et al.* Body mass index and the risk of development of end-stage renal disease in a screened cohort. *Kidney Int* 2004; **65**: 1870-6.
3. Hsu CY, McCulloch CE, Iribarren C, *et al.* Body mass index and risk for end-stage renal disease. *Ann Intern Med* 2006; **144**: 21-8.
4. Ejerblad E, Fored CM, Lindblad P, *et al.* Obesity and risk for chronic renal failure. *J Am Soc Nephrol* 2006; **17**: 1695-702.
5. Speckman RA, McClellan WM, Volkova NV, *et al.* Obesity is associated with family history of ESRD in incident dialysis patients. *Am J Kidney Di* 2006; **48**: 50-8.
6. Chen J, Muntner P, Hamm LL, *et al.* The metabolic syndrome and chronic kidney disease in U.S. adults. *Ann Intern Med* 2004; **140**: 167-74.
7. Pinto-Sietsma SJ, Navis G, Janssen WM, *et al.* A central body fat distribution is related to renal function impairment, even in lean subjects. *Am J Kidney Dis* 2003; **41**: 733-41.
8. Kwakernaak AJ, Zelle DM, Bakker SJ, *et al.* Central body fat distribution associates with unfavorable renal hemodynamics independent of body mass index. *J Am Soc Nephrol* 2013; **24**: 987-94.
9. Hricik DE. Metabolic syndrome in kidney transplantation: management of risk factors. *Clin J Am Soc Nephrol* 2011; **6**: 1781-5.
10. Pandya V, Rao A1, Chaudhary K1. Lipid abnormalities in kidney disease and management strategies. *World J Nephrol* 2015; **4**: 83-91.
11. Kuwahara S, Hosojima M, Kaneko R, *et al.* Megalin-Mediated Tubuloglomerular Alterations in High-Fat Diet-Induced Kidney Disease. *J Am Soc Nephrol* 2016; **27**: 1996-2008.
12. Jiang T, Wang Z, Proctor G, *et al.* Diet-induced obesity in C57BL/6J mice causes increased renal lipid accumulation and glomerulosclerosis via a sterol regulatory element-binding protein-1c-dependent *pathway. J Biol Chem* 2005; **280**: 32317-25.
13. Tonelli M, Moyé L, Sacks FM, *et al.* Cholesterol and Recurrent Events Trial Investigators. Effect of pravastatin on loss of renal function in people with moderate chronic renal insufficiency and cardiovascular disease. *J Am Soc Nephrol* 2003; **14**: 1605-13.
14. Bianchi S, Bigazzi R, Caiazza A, *et al.* A controlled, prospective study of the effects of atorvastatin on proteinuria and progression of kidney disease. *Am J Kidney Dis* 2003; **41**: 565-70.
15. Lee TM, Lin MS, Tsai CH, *et al.* Add-on and withdrawal effect of pravastatin on proteinuria in hypertensive patients treated with AT receptor blockers. *Kidney Int* 2005; **68**: 779-87.
16. Oyabu C, Hashimoto Y, Fukuda T, *et al.* Impact of low-carbohydrate diet on renal function: a meta-analysis of over 1000 individuals from nine randomised controlled trials. *Br J Nutr* 2016; **116**: 632-8.
17. Tirosh A, Golan R, Harman-Boehm I, *et al.* Renal function following three distinct weight loss dietary strategies during 2 years of a randomized controlled trial. *Diabetes Care* 2013; **36**: 2225-32.
18. Wahba IM, Mak RH. Obesity and obesity-initiated metabolic syndrome: mechanistic links to chronic kidney disease. *Clin J Am Soc Nephrol* 2007; **2**: 550-62.

19. de Vries AP, Ruggenenti P, Ruan XZ, *et al.* Fatty kidney: emerging role of ectopic lipid in obesity-related renal disease. *Lancet Diabetes Endocrinol* 2014; **2**: 417-26.
20. Platt FM, Boland B, van der Spoel AC. The cell biology of disease: lysosomal storage disorders: the cellular impact of lysosomal dysfunction. *J Cell Biol* 2012; **199**: 723-34.
21. Bakker PJ, Butter LM, Kors L, *et al.* Nlrp3 is a key modulator of diet-induced nephropathy and renal cholesterol accumulation. *Kidney Int* 2014; **85**: 1112-22.
22. Mizushima N. Methods for monitoring autophagy using GFP-LC3 transgenic mice. *Methods Enzymol* 2009; **452**: 13-23.
23. Settembre C, di Malta C, Polito VA, *et al.* TFEB Links Autophagy to Lysosomal Biogenesis. *Science* 2011; **332**: 1429–1433.
24. Ohshima T, Murray GJ, Swaim WD, *et al.* alpha-Galactosidase A deficient mice: a model of Fabry disease. *Proc Natl Acad Sci U S A*. 1997; **94**: 2540-4.
25. Ferraz MJ, Marques AR, Gaspar P, *et al.* Lyso-glycosphingolipid abnormalities in different murine models of lysosomal storage disorders. *Mol Genet Metab* 2016; **117**: 186-93.
26. van Eijk M, Aten J, Bijl N, *et al.* Reducing glycosphingolipid content in adipose tissue of obese mice restores insulin sensitivity, adipogenesis and reduces inflammation. *PLoS One* 2009; **4**: e4723.
27. Marques AR, Aten J, Ottenhoff R, *et al.* Reducing GBA2 Activity Ameliorates Neuropathology in Niemann-Pick Type C Mice. *PLoS One* 2015; **10**: e0135889.
28. Rampanelli E, Orsó E, Ochodnicky P, *et al.* Metabolic injury-induced NLRP3 inflammasome activation dampens phospholipid degradation. *Sci Rep* 2017; **7**: 2861.
29. McCluer RH, Williams MA, Gross SK, *et al.* Testosterone effects on the induction and urinary excretion of mouse kidney glycosphingolipids associated with lysosomes. *J Biol Chem* 1981; **256**: 13112-20.
30. Bligh EG, Dyer WJ. A rapid method of total lipid extraction and purification. *Can J Biochem Physiol* 1959; **37**: 911-7.
31. Liebisch G, Lieser B, Rathenberg J, *et al.* High-throughput quantification of phosphatidylcholine and sphingomyelin by electrospray ionization tandem mass spectrometry coupled with isotope correction algorithm. *Biochim Biophys Acta* 2004; **1686**: 108-17.
32. Liebisch G, Drobnik W, Reil M, *et al.* Quantitative measurement of different ceramide species from crude cellular extracts by electrospray ionization tandem mass spectrometry (ESI-MS/MS). *J Lipid Res* 1999; **40**: 1539–1546.
33. Baker DL, Desiderio DM, Miller DD, *et al.* Direct quantitative analysis of lysophosphatidic acid molecular species by stable isotope dilution electrospray ionization liquid chromatography-mass spectrometry. *Anal Biochem* 2001; **292**: 287-95.
34. Scherer M, Schmitz G, Liebisch G. High-throughput analysis of sphingosine 1-phosphate, sphinganine 1-phosphate, and lysophosphatidic acid in plasma samples by liquid chromatography-tandem mass spectrometry. *Clin Chem* 2009; **55**: 1218-22.
35. Scherer M, Schmitz G, Liebisch G. Simultaneous quantification of cardiolipin, bis(monoacylglycero)phosphate and their precursors by hydrophilic interaction LC-MS/MS including correction of isotopic overlap. *Anal Chem* 2010; **82**: 8794-9.
36. Ecker J, Scherer M, Schmitz G, *et al.* A rapid GC-MS method for quantification of positional and geometric isomers of fatty acid methyl esters. *J Chromatogr B Analyt Technol Biomed Life Sci* 2012; **897**: 98-104.
37. Baronas ET, Lee JW, Alden C, *et al.* Biomarkers to monitor drug-induced phospholipidosis.

Toxicol Appl Pharmacol 2007; **218**: 72-8.
38. Herzog K, Pras-Raves ML, Vervaart MA, *et al.* Lipidomic analysis of fibroblasts from Zellweger spectrum disorder patients identifies disease-specific phospholipid ratios. *J Lipid Res* 2016; **57**: 1447-54.
39. Rodriguez-Suarez E, Hughes C, Gethings L, *et al.* An Ion Mobility Assisted Data Independent LC-MS Strategy for the Analysis of Complex Biological Samples. *Curr Anal Chem* 2013; **9**: 199-211.
40. Distler U, Kuharev J, Navarro P, *et al.* Drift time-specific collision energies enable deep-coverage data-independent acquisition proteomics. *Nat Methods* 2014; **11**: 167-70.
41. Markmann S, Krambeck S, Hughes CJ, *et al.* Quantitative Proteome Analysis of Mouse Liver Lysosomes Provides Evidence for Mannose 6-phosphate-independent Targeting Mechanisms of Acid Hydrolases in Mucolipidosis II. *Mol Cell Proteomics* 2017; **16**: 438-450.
42. Fabregat A, Sidiropoulos K, Garapati P, *et al.* The Reactome pathway Knowledgebase. *Nucleic Acids Res* 2016; **44**: D481-7.
43. Conesa A, Götz S, García-Gómez JM, *et al.* Blast2GO: a universal tool for annotation, visualization and analysis in functional genomics research. *Bioinformatics* 2005; **21**: 3674-6.
44. Ashburner M, Ball CA, Blake JA, *et al.* Gene ontology: tool for the unification of biology. The Gene Ontology Consortium. *Nat Genet* 2000; **25**: 25-9.
45. van den Berg E, Pasch A, Westendorp WH, *et al*. Urinary sulfur metabolites associate with a favorable cardiovascular risk profile and survival benefit in renal transplant recipients. *J Am Soc Nephrol* 2014; **25**: 1303-12.
46. Eisenga MF, Kieneker LM, Soedamah-Muthu SS, *et al.* Urinary potassium excretion, renal ammoniagenesis, and risk of graft failure and mortality in renal transplant recipients. *Am J Clin Nutr* 2016; **104**: 1703-1711.
47. Gomes Neto AW, Sotomayor CG, Pranger IG, *et al*. Intake of Marine-Derived Omega-3 Polyunsaturated Fatty Acids and Mortality in Renal Transplant Recipients. *Nutrients* 2017; **9**: E363.
48. van den Berg E, Engberink MF, Brink EJ, *et al.* Dietary acid load and metabolic acidosis in renal transplant recipients. *Clin J Am Soc Nephrol* 2012; **7**: 1811-8.
49. Greenberg AS, Egan JJ, Wek SA, *et al.* Garty NB, Blanchette-Mackie EJ, Londos C. Perilipin, a major hormonally regulated adipocyte-specific phosphoprotein associated with the periphery of lipid storage droplets. *J Biol Chem* 1991; **266**: 11341-6.
50. Straub BK, Gyoengyoesi B, Koenig M, *et al.* Adipophilin/perilipin-2 as a lipid droplet-specific marker for metabolically active cells and diseases associated with metabolic dysregulation. *Histopathology* 2013; **62**: 617-31.
51. Praga M, Hernández E, Morales E, *et al.* Clinical features and long-term outcome of obesity-associated focal segmental glomerulosclerosis. *Nephrol Dial Transplant* 2001; **16**: 1790-8.
52. Kambham N, Markowitz GS, Valeri AM, *et al.* Obesity-related glomerulopathy: an emerging epidemic. *Kidney Int* 2001; **59**: 1498-509.
53. Chen HM, Li SJ, Chen HP, *et al.* Obesity-related glomerulopathy in China: a case series of 90 patients. *Am J Kidney Dis* 2008; **52**: 58-65.
54. Schmitz G, Müller G. Structure and function of lamellar bodies, lipid-protein complexes involved in storage and secretion of cellular lipids. *J Lipid Res* 1991; **32**: 1539-70.
55. Carmona-Gutierrez D, Hughes AL, Madeo F, *et al.* The crucial impact of lysosomes in aging and longevity. *Ageing Res Rev* 2016; **32**: 2-12.

56. Pankiv S, Clausen TH, Lamark T, *et al.* p62/SQSTM1 binds directly to Atg8/LC3 to facilitate degradation of ubiquitinated protein aggregates by autophagy. *J Biol Chem* 2007; **282**: 24131-45.
57. Liu K, Czaja MJ. Regulation of lipid stores and metabolism by lipophagy. *Cell Death Differ* 2013; **20**: 3-11.
58. Sardiello M, Palmieri M, di Ronza A, *et al.* A gene network regulating lysosomal biogenesis and function. *Science* 2009; **325**: 473-7.
59. Palmieri M, Impey S, Kang H, *et al.* di Ronza A, Pelz C, Sardiello M, Ballabio A. Characterization of the CLEAR network reveals an integrated control of cellular clearance pathways. *Hum Mol Genet* 2011; **20**: 3852-66.
60. Horton JD, Goldstein JL, Brown MS. SREBPs: activators of the complete program of cholesterol and fatty acid synthesis in the liver. *J Clin Invest* 2002; **109**: 1125-31.
61. Horton JD, Shah NA, Warrington JA, *et al.* Combined analysis of oligonucleotide microarray data from transgenic and knockout mice identifies direct SREBP target genes. *Proc Natl Acad Sci U S A* 2003; **100**: 12027-32.
62. Ma X, Chen Z, Hua D, *et al.* Essential role for TrpC5-containing extracellular vesicles in breast cancer with chemotherapeutic resistance. *Proc Natl Acad Sci U S A* 2014; **111**: 6389-94
63. Lu F, Liang Q, Abi-Mosleh L, *et al*. Identification of NPC1 as the target of U18666A, an inhibitor of lysosomal cholesterol export and Ebola infection. *Elife* 2015; **4**: e12177.
64. Tang Y, Leao IC, Coleman EM, *et al.* Deficiency of niemann-pick type C-1 protein impairs release of human immunodeficiency virus type 1 and results in Gag accumulation in late endosomal/lysosomal compartments. *J Virol* 2009; **83**: 7982-95.
65. Peake KB, Vance JE. Defective cholesterol trafficking in Niemann-Pick C-deficient cells. *FEBS Lett* 2010; **584**: 2731-9.
66. Christensen EI, Birn H. Megalin and cubilin: multifunctional endocytic receptors. *Nat Rev Mol Cell Biol* 2002; **3**: 256-66.
67. Kuwahara S, Hosojima M, Kaneko R, *et al.* Megalin-Mediated Tubuloglomerular Alterations in High-Fat Diet-Induced Kidney Disease. *J Am Soc Nephrol* 2016; **27**: 1996-2008.
68. Pfeifer SM, Furth EE, Ohba T, *et al.* Sterol carrier protein 2: a role in steroid hormone synthesis? *J Steroid Biochem Mol Biol* 1993; **47**: 167-72.
69. Puglielli L, Rigotti A, Greco AV, *et al.* Sterol carrier protein-2 is involved in cholesterol transfer from the endoplasmic reticulum to the plasma membrane in human fibroblasts. *J Biol Chem* 1995; **270**: 18723-6.
70. Nakasone N, Nakamura YS, Higaki K, *et al.* Endoplasmic reticulum-associated degradation of Niemann-Pick C1: evidence for the role of heat shock proteins and identification of lysine residues that accept ubiquitin. *J Biol Chem* 2014; **289**: 19714-25.
71. Dall E, Brandstetter H. Structure and function of legumain in health and disease. *Biochimie* 2016; **122**: 126-50.
72. Kocher O, Krieger M. Role of the adaptor protein PDZK1 in controlling the HDL receptor SR-BI. *Curr Opin Lipidol* 2009; **20**: 236-41.
73. Mahley RW, Rall SC Jr. Apolipoprotein E: far more than a lipid transport protein. *Annu Rev Genomics Hum Genet* 2000; **1**: 507-37.
74. Settembre C, Fraldi A, Medina DL, Ballabio A. Signals from the lysosome: a control centre for cellular clearance and energy metabolism. *Nat Rev Mol Cell Biol* 2013; **14**: 283-96.

75. Appelqvist H, Wäster P, Kågedal K, *et al.* The lysosome: from waste bag to potential therapeutic target. *J Mol Cell Biol* 2013; **5**: 214-26.
76. Ridsdale R, Na CL, Xu Y, *et al.* Comparative proteomic analysis of lung lamellar bodies and lysosome-related organelles. *PLoS One* 2011; **6**: e16482.
77. Raymond AA, Gonzalez de Peredo A, Stella A, *et al.* Lamellar bodies of human epidermis: proteomics characterization by high throughput mass spectrometry and possible involvement of CLIP-170 in their trafficking/secretion. *Mol Cell Proteomics* 2008; **7**: 2151-75.
78. Hu ZZ, Valencia JC, Huang H, *et al.* Comparative Bioinformatics Analyses and Profiling of Lysosome-Related Organelle Proteomes. *Int J Mass Spectrom* 2007; **259**: 147-160.
79. D'Aquila T, Sirohi D, Grabowski JM, *et al.* Characterization of the proteome of cytoplasmic lipid droplets in mouse enterocytes after a dietary fat challenge. *PLoS One* 2015; **10**: e0126823.
80. Brasaemle DL, Dolios G, Shapiro L, *et al.* Proteomic analysis of proteins associated with lipid droplets of basal and lipolytically stimulated 3T3-L1 adipocytes. *J Biol Chem* 2004; **279**: 46835-42.
81. Fujimoto Y, Itabe H, Sakai J, *et al.* Identification of major proteins in the lipid droplet-enriched fraction isolated from the human hepatocyte cell line HuH7. *Biochim Biophys Acta* 2004; **1644**: 47-59.
82. Ehnholm C. Cellular Lipid Metabolism. Springer: Verlag Berlin Heidelberg, 2009: 27-71.
83. Bjørkøy G, Lamark T, Brech A, *et al.* p62/SQSTM1 forms protein aggregates degraded by autophagy and has a protective effect on huntingtin-induced cell death. *J Cell Biol* 2005; **171**: 603-14.
84. Schmitz G, Grandl M. Endolysosomal phospholipidosis and cytosolic lipid droplet storage and release in macrophages. *Biochim Biophys Acta* 2009; **1791**: 524-39.
85. Solomon VR, Lee H. Chloroquine and its analogs: a new promise of an old drug for effective and safe cancer therapies. *Eur J Pharmacol* 2009; **625**: 220-33.
86. Orsó E, Grandl M, Schmitz G. Oxidized LDL-induced endolysosomal phospholipidosis and enzymatically modified LDL-induced foam cell formation determine specific lipid species modulation in human macrophages. *Chem Phys Lipids* 2011; **164**: 479-87.
87. Han WK, Bailly V, Abichandani R, *et al.* Kidney Injury Molecule-1 (KIM-1): a novel biomarker for human renal proximal tubule injury. *Kidney Int* 2002; **62**: 237-44.
88. Lee SY, Kim SI, Choi ME. Therapeutic targets for treating fibrotic kidney diseases. *Transl Res* 2015; **165**: 512-30.
89. Nosratola DV. Disorders of lipid metabolism in nephrotic syndrome: mechanisms and consequences. *Kid Int* 2016; **90**: 41-52.
90. Liu N, Tengstrand EA, Chourb L, *et al.* Di-22:6-bis(monoacylglycerol)phosphate: A clinical biomarker of drug-induced phospholipidosis for drug development and safety assessment. *Toxicol Appl Pharmacol* 2014; **279**: 467-76.
91. Prasad GV. Metabolic syndrome and chronic kidney disease: Current status and future directions. *World J Nephrol* 2014; **3**: 210-9.
92. Zhou XJJ, Laszik ZG, Nadasdy T, D'Agati VD. Silva's Diagnostic Renal Pathology (2nd edn). Cambridge University Press: Cambridge, 2017; 1-56.
93. Christoph JO, Mathias F, Elisabeth G. Alterations in lysosomal enzymes of the proximal tubule in gentamicin nephrotoxicity. *Kidney Int* 1991; **39**: 639-646.
94. Olbricht CJ, Cannon JK, Garg LC, *et al.* Tisher CC. Activities of cathepsins B and L in isolated nephron segments from proteinuric and nonproteinuric rats. *Am J Physiol* 1986; **250**: F1055-

62.
95. Olbricht CJ, Cannon JK, Tisher CC. Cathepsin B and L in nephron segments of rats with puromycin aminonucleoside nephrosis. *Kidney Int* 1987; **32**: 354-61.
96. Madsen KM1, Park CH. Lysosome distribution and cathepsin B and L activity along the rabbit proximal tubule. *Am J Physiol* 1987; **253**: F1290-301.Skeldon AM, Faraj M, Saleh M. Caspases and inflammasomes in metabolic inflammation. *Immunol Cell Biol* 2014; **92**: 304-13.
97. Muntner P, Coresh J, Smith JC, *et al.* Plasma lipids and risk of developing renal dysfunction: the atherosclerosis risk in communities study. *Kidney Int* 2000; **58**: 293-301.
98. Hariri M, Milane G, Guimond MP, *et al*. Biogenesis of multilamellar bodies via autophagy. *Mol Biol Cell* 2000; **11**: 255–268.
99. Rajat S, Susmita K, Yongjun W, *et al.* Autophagy regulates lipid metabolism. *Nature* 2009; **458**: 1131–1135.
100. Satriano J and Sharma K. Autophagy and metabolic changes in obesity-related chronic kidney disease. *Nephrol Dial Transplant* 2013; **28**: iv29–iv36.
101. Settembre C, De Cegli R, Mansueto G, *et al*. TFEB controls cellular lipid metabolism through a starvation-induced autoregulatory loop. *Nat Cell Biol* 2013; **15**: 647-58.
102. Strable MS, Ntambi JM. Genetic control of de novo lipogenesis: role in diet-induced obesity. *Crit Rev Biochem Mol Biol* 2010; **45**: 199-214.
103. Chagnac A, Weinstein T, Herman M, *et al*. The effects of weight loss on renal function in patients with severe obesity. *J Am Soc Nephrol* 2003; **14**: 1480-6.
104. Declèves AE, Sharma K. Obesity and kidney disease: differential effects of obesity on adipose tissue and kidney inflammation and fibrosis. *Curr Opin Nephrol Hypertens* 2015; **24**: 28-36.
105. Gallala HD, Sandhoff K. Biological function of the cellular lipid BMP-BMP as a key activator for cholesterol sorting and membrane digestion. *Neurochem Res* 2011; **36**: 1594-1600.
106. Thompson KL, Zhang J, Stewart S, *et al*. Comparison of urinary and serum levels of di-22:6-bis(monoacylglycerol)phosphate as noninvasive biomarkers of phospholipidosis in rats. *Toxicol Lett* 2012; **213**: 285-91.
107. Declèves AE, Sharma K. Novel targets of antifibrotic and anti-inflammatory treatment in CKD. *Nat Rev Nephrol* 2014; **10**: 257-67.
108. Declèves AE, Mathew AV, Cunard R, *et al*. AMPK mediates the initiation of kidney disease induced by a high-fat diet. *J Am Soc Nephrol* 2011; **22**: 1846-55.
109. Deji N, Kume S, Araki S, *et al*. Structural and functional changes in the kidneys of high-fat diet-induced obese mice. *Am J Physiol Renal Physiol* 2009; **296**: F118-26.
110. Declèves AE, Zolkipli Z, Satriano J, *et al*. Regulation of lipid accumulation by AMK-activated kinase in high fat diet-induced kidney injury. *Kidney Int* 2014; **85**: 611-623.
111. Wang XX, Jiang T, Shen Y, *et al*. The farnesoid X receptor modulates renal lipid metabolism and diet-induced renal inflammation, fibrosis, and proteinuria. *Am J Physiol Renal Physiol* 2009; **297**: F1587-96.
112. Sun L, Halaihel N, Zhang W, *et al*. Role of sterol regulatory element-binding protein 1 in regulation of renal lipid metabolism and glomerulosclerosis in diabetes mellitus. *J Biol Chem* 2002; **277**: 18919-27.
113. Yamamoto T, Takabatake Y, Takahashi A, *et al*. High-fat diet-induced lysosomal dysfunction and impaired autophagic flux contribute to lipotoxicity in the kidney. *J Am Soc Nephrol* 2017; **28**: 1534-1551.
114. Maceyka M, Spiegel S. Sphingolipid metabolites in inflammatory disease. *Nature* 2014; **510**:

58-67.
115. Arana L, Gangoiti P, Ouro A, *et al*. Trueba M, Gómez-Muñoz A. Ceramide and ceramide 1-phosphate in health and disease. *Lipids Health Dis*. 2010; **9**:15.
116. Hammer S, de Vries AP, de Heer P, *et al*. Metabolic imaging of human kidney triglyceride content: reproducibility of proton magnetic resonance spectroscopy. *PLoS One* 2013; **8**: e62209.

Figure legends

Figure 1. Accumulation of polar lipids (phospholipids) and free cholesterol in murine proximal tubular epithelial cells upon Western-type diet feeding. (A) PAS-D-stained renal sections of mice fed a control diet (CD) or Western-type diet (WD), 20 × magnification. (B) Quantification of tubular vacuolization in PAS-D-stained kidney sections of CD- and WD-fed mice: number of vacuolized tubules per high-power field (HPF, 20 ×). (C) Perilipin-2 staining in CD and WD kidneys sections (20 × magnification, 100 × magnification far-right image). (D) Nile red and (E) Filipin staining of renal sections for detection of phospholipids and free cholesterol, respectively, in kidneys of CD- and WD-fed mice (D and E: 20 × and 40 × magnification, respectively). (F) Lipidomics analysis (ESI-MS/MS) of renal lipid content: free-cholesterol (FC), cholesterol-esters (CE), fatty acids (FA), bismonoacylglycerophosphate (BMP), phosphatidylglycerol (PG), lysophosphatidylglycerol (LPG), phosphatidic acid (PA), cardiolipin (CL), sphingomyelin (SPM), ceramide, ceramide-1-phosphate (Cer-1-P), lactosylceramide (LacCer), glucosylceramide (GluCer), sphingosine, sphinganine, phosphatidylcholine (PC), lysophosphatidylcholine (LPC), phosphatidylethanolamine (PE), phosphatidylinositol (PI), phosphatidylserine (PS), plasmogens. (B, F) Data shown as mean ± s.e.m.; *P<0.05, ***P<0.001.

Figure 2. Features of acquired lysosomal storage disease in kidneys exposed to metabolic overloading. (A) Transmission electron microscopy (TEM) images of control diet (CD) and Western-type diet (WD) murine kidneys (upper panel): L, luminal space, MLB, multilamellar bodies, N, nucleus, scale bar 10/2 µm. Staining for LIMP-2 and CD63 in CD and WD kidneys sections (20 × magnification, 40 × magnification far-right column). (B) Images of renal sections of WD-fed mice stained for p62 (40 × magnification; asterisk= positive vacuolar membrane) and of GFP-LC3/LIMP-2 double-stained kidney sections from GFP-LC3 transgenic mice upon WD feeding (100 × magnification; LIMP-2 = red;

GFP = blue, asterisk = co-localization, purple). (C) Counts of GFP-LC3 puncta per proximal tubule in CD and WD kidneys. (D) mRNA expression of genes related to lysosome function (left graph) and lipogenic pathways (right graph) in laser-dissected vacuolar tubules and respective controls from mice fed a WD and CD, respectively. Values normalized to control. (E) Positive staining for LDLR, oxidized lipoproteins (oxLP) and lipoproteins (LP) in kidneys of WD-fed mice (20 × magnification). Data shown as mean ± s.e.m.; *P<0.05, **P<0.01, ***P<0.001.

Figure 3. Proteomics analysis of MLBs isolated from murine kidneys and urine upon metabolic overloading. (A) TEM analysis of urine of mice on Western-type diet (WD); scale bars 10/2 µm. (B) Western blot for detection of exosome marker Flotillin-2 in total cell lysates and cell-derived supernatant in control and U18666A-treated immortalized murine tubular epithelial cells (IMM-PTEC). (C) Most abundant proteins found in MLBs isolated from both kidney tissue and urine of WD-fed mice and U18666A-treated IMM-PTEC. Proteins shown after selecting the 50 proteins with the highest ppm (relative LC-MS abundance) independently in the protein list derived from proteomic analysis of kidney, urine and IMMP-TEC MLBs. (D) Graph showing the frequency of protein origin among all intracellular organelles and extracellular exosomes. The proteins considered for analysis are the most abundant proteins shown in (C).

Figure 4. Hierarchical cluster and frequency analysis to compare the proteomic profiles of murine kidney MLBs (our data), lysosome-related organelles (LROs) [78], lung MLBs [76], epidermis MLBs [77], lipid droplets (Lds) from enterocytes [79], adipocytes [80], and hepatocytes [81].

Figure 5. Interference with cholesterol trafficking and oxysterol treatment are responsible for MLB formation, disruption of lysosome homeostasis and induction of genes regulating cholesterogenesis. (A) TEM images showing the formation of MLBs after *in vitro* incubation of immortalized murine tubular epithelial cells (IMM-PTEC) with U18666A, oxidized low density lipoproteins (oxLDL), and oxysterol 7-ketocholesterol (7-KC). Asterisks indicate cellular MLBs localization. (B) Fluorescence microscopy (FM) images, in which phospholipidosis and LIMP-2 are detected in control and IMM-PTEC cells stimulated with U18666A/oxLDL/7KC; nuclei = blue, phospholipidosis = red, LIMP-2 = green, co-localization = yellow; 100 × magnification. (C) Increase of lysosomal pH after incubation of IMM-PTEC with U18666A, oxLDL, 7KC, and chloroquine (CQ, positive controls). (D) FM images of control and U18666A-stimulated human PTEC HK2 cells, showing cellular accumulation of phospholipids, cholesterol (filipin staining) and BMP; nuclei = blue, phospholipidosis = red, cholesterol = blue, BMP = green; 10 × magnification. (E) FM images of U18666A-stimulated HK2 cells, showing phospholipidosis and BMP distribution; nuclei = blue, phospholipidosis = red, BMP = green, co-localization = yellow; 100 × magnification. (F) Gene expression of the transcription factor *Srebp2,* its target genes *Ldlr* and *Hmgcr*, and lysosomal phospholipase A2 (*Lpla2*) in control and U18666A-stimulated IMM-PTEC. Values normalized to control. Data shown as mean ± s.e.m.; *P<0.05, **P<0.01, ***P<0.001.

Figure 6. Diet-mediated lipid overload of tubular cells associates with an inflammatory milieu, collagen deposition, and reduced specialized transporter expression. (A) Immunostaining of renal sections from control diet (CD)- and Western-type diet (WD)-fed mice for visualization of the apical SGLT2 transporter, tubular damage marker KIM-1, macrophage infiltration, and collagen type III deposition; 20 × magnification. (B, C) Quantitative gene expression analysis for membrane

transporters (SGLT2, ATP1A1), chemokine MCP-1, damage marker KIM-1, fibrogenic markers TGF-β and CTGF in (B) murine renal tissues and (C) IMM-PTEC. Values normalized to control. (D) Electrolyte concentration (sodium, potassium and chloride) in urine of mice fed CD or WD; values normalized for urinary creatinine (nmol/mmol). (E) Representative images of renal biopsy from obese hypercholesterolaemic patients. Conventional staining with acidophilic dye toluidine blue (left upper image) and immunostaining for LIMP-2 revealing the presence of vacuoles within proximal tubular cells and the expression of LIMP-2 at the vacuolar membrane, respectively; 20 × magnification. Immunofluorescence for visualization of the lysosomal glycerophospholipid BMP within TEC; 100 × magnification. TEM images of human tubular cells harbouring MLBs (indicated by asterisks), scale bar 5 and 1 µm. (F) Quantitative lipidomics analysis: di-docosahexaenoyl (22:6) bis(monoacylglycerol) phosphate (di-22:6-BMP) content in human urine specimens; *n* = 21. (G) Spearman correlation between total albumin and di-22:6-BMP urinary concentrations; human urine specimens; *n* = 21. Data shown as mean ± s.e.m.; *P<0.05, **P<0.01, ***P<0.001.

SUPPLEMENTARY MATERIAL ONLINE

Supplementary materials and methods YES

Supplementary figure legends YES

Figure S1. PAS-D stained renal sections of wild-type mice fed a control diet (CD) or Western-type diet (WD)

Figure S2. Kidney specimens from various mouse models of acquired lysosomal storage disease, obesity and aging to compare MLB formation

Figure S3. Isolation of MLBs by sucrose gradient-centrifugation and proteomics data analysis

Figure S4. MLB proteins clustered by function and location

Figure S5. GO terms and KEGG pathway annotation of 7 distinct proteomics datasets

Figure S6. Transmission electron microscopy (TEM) images of kidney biopsies from patients with nephrotic syndrome

Table S1. Comparison among proteomes of kidney/lung/epidermis-derived MLBs, lysosome-related organelles (LROs), and lipid droplets (LDs) from enterocytes, adipocytes and hepatocytes

Table S2. Primer sequences

Excel spreadsheet file S1.

Excel spreadsheet file S2.

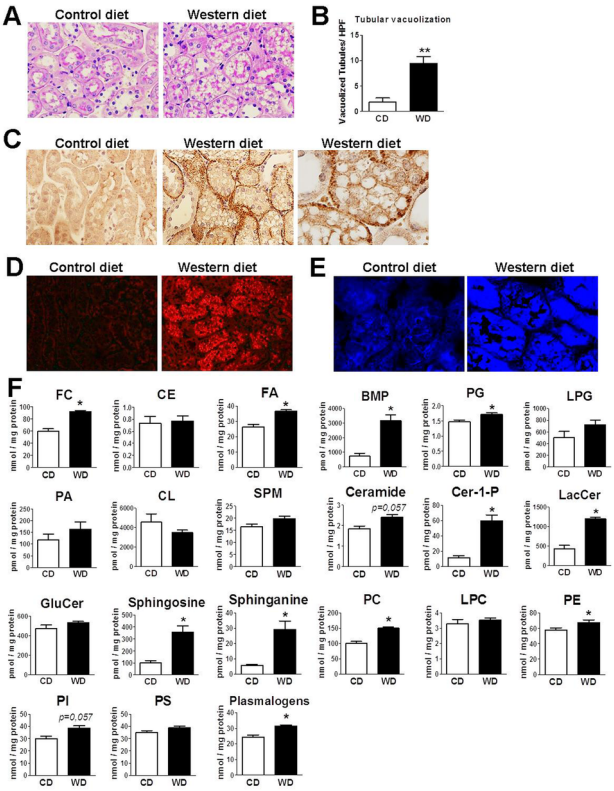

PATH_5150_F1.tif

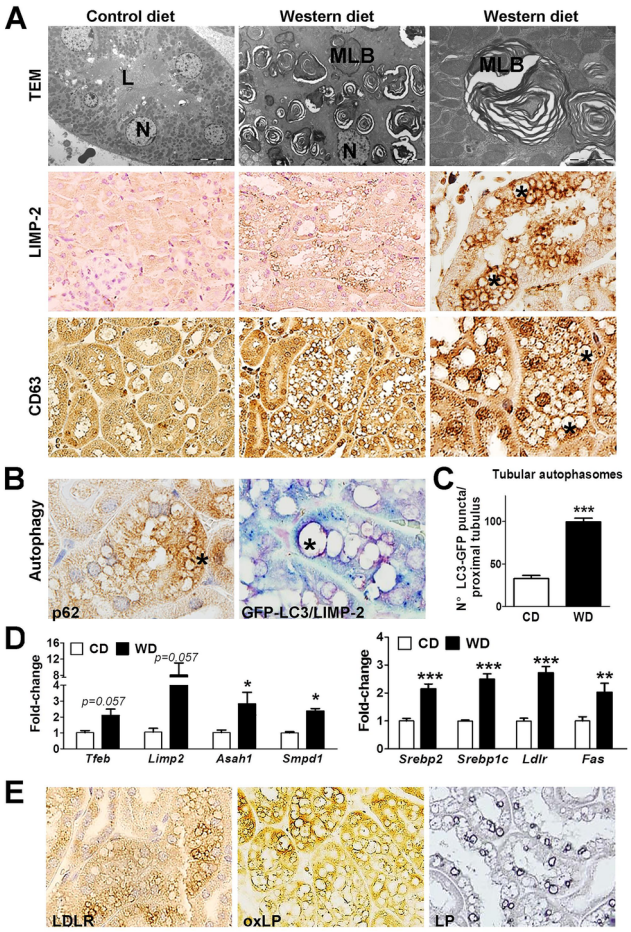

PATH_5150_F2.tif

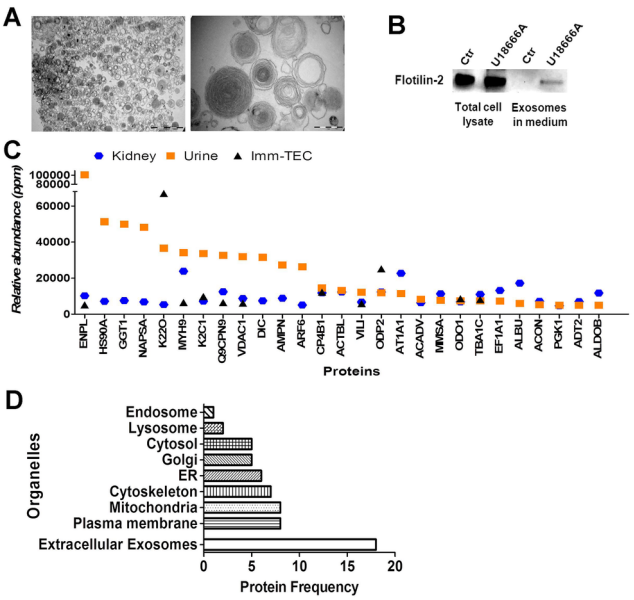

PATH_5150_F3.tif

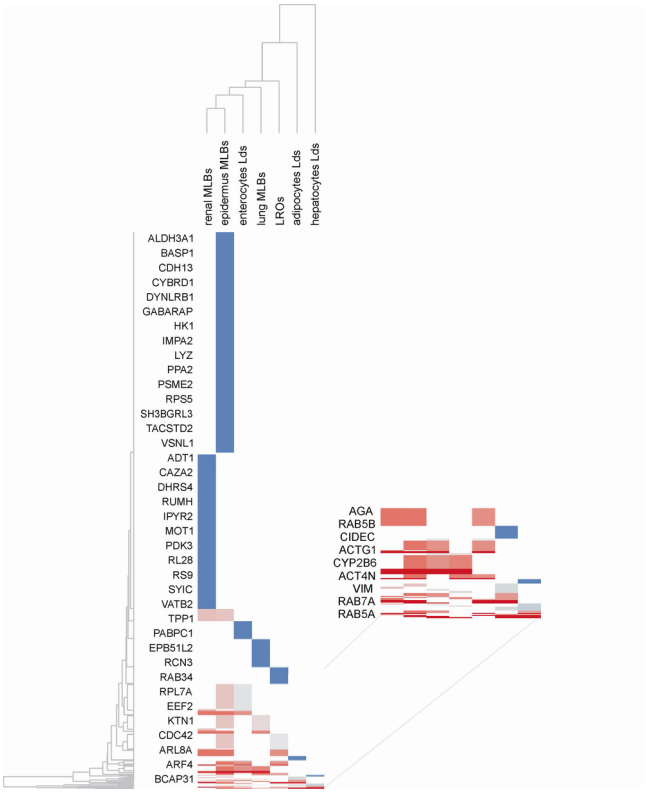

PATH_5150_F4.tif

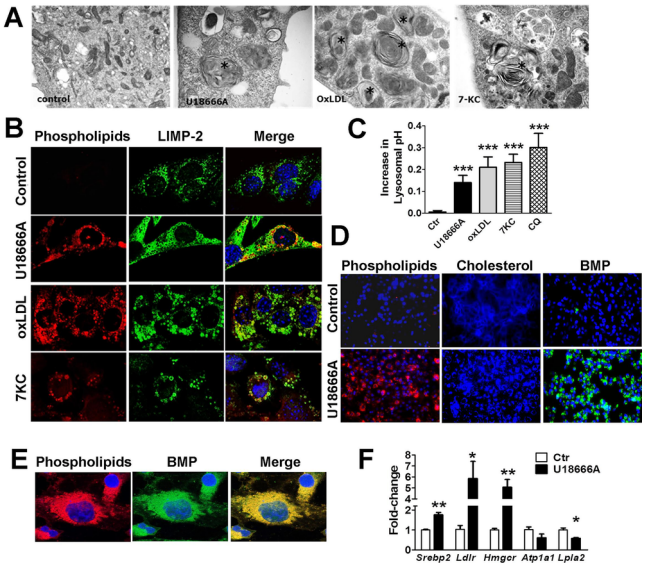

PATH_5150_F5.tif

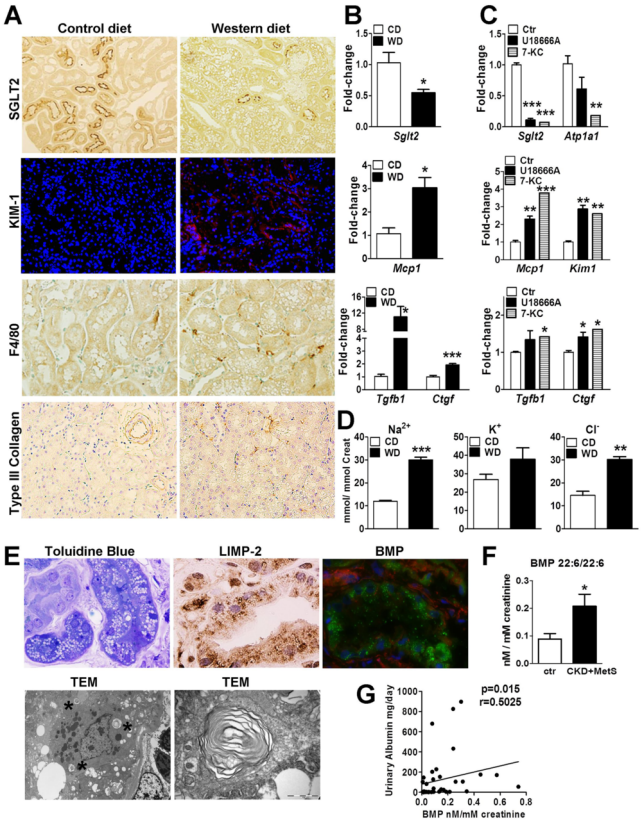

PATH_5150_F6.tif